Burckel *et al.*
Journal of Translational Medicine (2025) 23:360
https://doi.org/10.1186/s12967-025-06377-7

Journal of Translational Medicine

RESEARCH

Open Access

Distinct immune responses to proton and photon radiotherapy: implications for anti-PD-L1 combination therapy in colorectal cancer

Hélène Burckel[1,2*], Anaïs Nicol[1,2], Carole Mura[1,2], Marc Rousseau[3], Jolie Bou-Gharios[1,2], Lisa Froidurot[4], Corentin Richard[5], Véronique Morgand[4], Pierre-Antoine Laurent[4], Emeric Limagne[6,7], Romain Boidot[5], Georges Noël[1,2,8] and Céline Mirjolet[4,6]

Abstract

Background Ionizing radiation can influence the antitumor immune response, either activating or suppressing the immune system depending on the tumor type and radiotherapy modality. While photon radiation (RT) combined with immunotherapy (IT) is widely studied in clinical trials, proton radiation (PT) combined with IT has not been thoroughly investigated in clinical or preclinical studies despite its radiobiological advantages. This study aims to explore the immune effects of a hypofractionated PT scheme compared to RT and its efficacy with anti-PD-L1 immunotherapy.

Methods Balb/c mice bearing subcutaneous CT26 colon tumors were treated with RT or PT, delivered with 3×8 Gy. Seven days post-treatment, transcriptomic analysis and immune response assessments to characterize lymphoid cells, myeloid cells, and PD-L1 expression were performed. Tumor growth was monitored to evaluate the efficacy of combining RT or PT with anti-PD-L1 IT.

Results The RNA sequencing analysis demonstrated an overexpression of genes involved in the interferon type I pathway after both RT and PT. Tumor microenvironment analysis showed enhanced immune cell infiltration in tumors after both treatments. Immunoactivating cells infiltration was observed, with LT CD8 + cells infiltration after both RT and PT, more significantly after RT. NK and TAM1 cells infiltrated only after RT. Immunosuppressive cell populations were induced by PT, including MDSCs, while Tregs infiltrated both RT and PT treated tumors. PD-L1 expression was significantly induced only by RT. The combination of anti-PD-L1 with RT or PT resulted in tumor growth delay compared to RT or PT alone, with a significant survival benefit observed only after the combination of RT and IT.

Conclusions This study demonstrates that hypofractionated RT and PT induced both similar and significantly distinct immune responses. PT triggers a stronger immunosuppressive response than RT. Optimizing the combination of PT with IT, including dose, fractionation, and sequencing is crucial for improving treatment efficacy.

Keywords Proton therapy, Photon, Radiotherapy, Immune response, Preclinical model, Colorectal cancer

*Correspondence:
Hélène Burckel
h.burckel@icans.eu
Full list of author information is available at the end of the article

Introduction

Radiation therapy using photons (RT) is a pivotal cancer treatment, prescribed in both curative and palliative contexts [1, 2]. The primary goal of RT is to induce significant DNA double-strand breaks, leading to genomic instability and eventual cell death [3]. Rigorous investigations in preclinical and clinical domains provide substantial evidence supporting the well-established concept that ionizing radiation can modulate the immune tumor microenvironment (TME) [4–6].

RT can induce immunogenic cell death (ICD) by triggering the release of tumor neoantigens, the translocation of calreticulin to the cell surface, the extracellular release of high-mobility group protein B1 (HMGB1), and the secretion of adenosine triphosphate (ATP) [7]. These processes are essential for the activation of antigen-presenting cells, such as dendritic cells (DCs), and priming of effector T cells. Furthermore, RT induces the release of double-stranded DNA into the cytoplasm, which plays a pivotal role in activating the cGAS-STING pathway and promoting the transcription of type I interferon, a key factor in DC activation [8–12]. This process enables immune cells to migrate to distant tumors, thereby contributing to the regulation of metastasis through the abscopal effect [13, 14]. Additionally, RT enhances the recruitment of natural killer (NK) cells, cytotoxic CD8 + T cells and type 1 T helper (Th1) cells to the TME through the induction of chemokines like CXCL9, CXCL10, and CXCL16 [15–18].

Conversely, RT can promote processes that inhibit the immune system. For instance, RT can stimulate the accumulation of cells within the TME that suppress the immune response, such as regulatory T cells (Treg), myeloid-derived suppressor cells (MDSC), and tumor-associated macrophages 2 (TAM2). Additionally, RT can trigger the expression of PD-1 ligand (PD-L1) on both tumor and immune cells, as well as an increase in immune checkpoint receptors (PD-1, TIGIT, TIM-3) on tumor-infiltrating lymphocytes (TILs), or PD-L1 on the surface of cancer cells, thereby limiting the activation and function of CD8 T cells [19–25].

Immunotherapy (IT) can effectively inhibit specific immunosuppressive mechanisms. Consequently, the combination of RT with IT has been extensively explored in preclinical studies and remains a central focus in numerous ongoing clinical trials. These trials involve the implication of diverse novel immunotherapeutic agents currently in development, providing a range of options for tailoring combination approaches [26–30]. The investigation of these innovative combinations holds promise, particularly in addressing indications related to solid tumors, especially in the context of metastasis.

The intricate equilibrium between the immunoactivating and immunosuppressive effects is complex, with underlying mechanisms influenced by several parameters, including the radiation type (particles used, LET, etc.), radiation absorbed dose, irradiated volume, fractionation regimen, specifically the dose per fraction and the timing of IT administration [11, 29, 31–35].

The Bragg peak of PT enables more precise radiation energy delivery to tumors, with its advantageous ballistic characteristics and its Linear Energy Transfer (LET), in contrast to the exit radiation dose of conventional RT [36, 37]. Notably, PT allows the avoidance of tissues located beyond the Bragg peak. In clinical settings, the average LET for PT is relatively modest (~ 2 keV/µm), reaching a maximum of approximately 8 keV/µm at the distal edge of the spread-out Bragg peak (SOBP), which, while modestly elevated, remains slightly higher than that of conventional photons (~ 0.5 keV/µm).

The precision of PT, particularly its ability to target tumor tissue while sparing healthy tissue, can enhance antitumor immune responses. By preserving surrounding lymph nodes, PT may reduce radio-induced lymphopenia and promote CD8 + activation. Additionally, sparing organs like the intestine can promote antitumor immunity through monocyte infiltration into the TME. In contrast, gut irradiation increases intestinal permeability and gastrointestinal damage, potentially redirecting monocytes away from the tumor, which could impair the immune response [38].

Combining PT with IT has gained interest in the field of cancer treatment, as PT is supposed to offer distinct advantages when compared to RT. Indeed, the enhanced precision of PT in tumor targeting decreases damage to surrounding healthy tissues and organs at risk (OAR), thereby reducing potential immunosuppressive effects associated with collateral radiation damages. Moreover, by sparing healthy tissues from radiation, PT can reduce overall absorbed radiation doses outside the tumor volume. For example, by reducing radiation-induced damage to nearby lymph nodes and minimizing lymphopenia, PT could play a key role in preserving immune cells in the bloodstream [39], potentially lowering systemic inflammation and enhancing the immune response for a more effective IT. As previously presented, PT may induce distinct biological effects compared to RT, potentially enhancing immunogenic cell death and promoting a stronger immune response against cancer cells [39]. Therefore, combining PT with IT could result in a synergistic therapeutic effect.

Given the recognized advantages of combining IT to RT, it would be valuable to explore the effects of combining IT and PT. However, research on the immune response to PT remains limited, highlighting the need for

further investigation in this area. Notably, some ongoing or completed clinical trials are investigating the synergistic effects of PT and IT, using the same protocols as RT and IT trials, despite limited knowledge of the potential differences in immune effects induced by PT versus RT.

The objective of our project is to assess and compare the influence of a radiation hypofractionation scheme involving either photons or protons on immune response. Additionally, we aim to evaluate the effectiveness of this hypofractionation regimen when combined with an anti-programmed death-ligand 1 (anti-PD-L1) immunotherapy protocol, using a consistent preclinical model.

Methods

Cell culture

CT26 mouse colon carcinoma cell line was purchased from American Type Culture Collection. CT26 cells were cultured in RPMI 1640 (Dutscher, France) media supplemented with 10% fetal bovine serum (PAN Biotech GmbH, Aidenbach, Germany). Cells growth conditions were 37 °C temperature in a humidified atmosphere containing 5% CO_2 and 95% humidity.

In vivo *experiments*

The PT and RT studies were conducted in two separate animal facilities, thus distinct control mice groups were assigned to each treatment group (PT and RT) in both facilities. Tumor grafting was assessed as previously described [40]. CT26 cells (5.10^5) were suspended in 100 µl of NaCl, and a subcutaneous injection was performed in the right flank of immunocompetent 8-week BALB/c female mice (Charles River Laboratories, Saint Germain Nuelles, France). Tumor size was followed until tumor volume (TV) reached the limit point of 1500 mm^3 as previously described [40]. Mice were randomized ten days after grafting to obtain a uniform mean tumor volume in each group with 180 ± 20 mm^3. In the survival study, mice were sacrificed after reaching the end point (tumor size $\geq$ 1500 mm^3) or 50 days after treatment (n = 10 mice). Some mice were euthanized after 7 days for RNA-Seq analysis (n = 4–5 mice) and for immunomonitoring experiments (n = 5–8 mice). Mice were sacrificed by cervical dislocation after general anesthesia (2% isoflurane) as recommended. All animal experiments were carried out according to standard approved protocols in accordance with the French legislation on the use of laboratory animals (EU Directive 2010/63/EU for animal experiments), and with ethical rules for the care and use of animals for research from the small animal ethics committee (C2ea Grand Campus n°105 and C2ea Cremeas n°35, C2ea Icomech n°38) and the French Ministries of Research and Agriculture (APAFIS#13961–2018022215413276 v2, APAFIS#22350–201910091738155 v2 and APAFIS#8235-201612161350414_v1). All animal protocols comply with the ARRIVE guidelines.

Treatments

Tumors were irradiated under anesthesia (isoflurane 2%, Minerve system, France) 10 days after xenograft formation with 3 fractions of 8 Gy (3 × 8 Gy) administered daily.

Photon irradiations were achieved using a small animal irradiator (SARRP, Xstrahl, UK) with 225 kV X-ray at a dose rate of 3.1 Gy/min. Ballistic used two opposite beams focusing on the tumor and totally avoiding the mouse's healthy organs, as described previously [41].

Proton beam irradiation was delivered with an energy beam of 25 MeV extracted from the Cyclotron (Cyclotron pour la Recherche et l'Enseignement, CYRCé platform, Institut Pluridisciplinaire Hubert Curien, Strasbourg, France). For proton radiation, tumor-bearing mice were irradiated in direct contact with the collimator using a scattering spread-out Bragg peak, as previously described [42, 43], at the same dose rate as X-rays (3.1 Gy/min).

Immunotherapy. Intra-peritoneal injections of Immunoglobulin G (IgG) (BioXcel, USA) and anti-PD-L1 (BioXcel) were performed 3 times per week for 3 weeks, starting the first day of irradiation, at a dose of 10 mg/kg per injection.

Flow cytometry

The effect of the immune response after RT and PT was analyzed by flow cytometry 7 days after treatment as previously described [40]. Tumors were dissected and then dissociated using a mouse tumor dissociation kit (Miltenyi Biotech). Myeloid cell infiltration was assessed by flow cytometry with tumor cells (10^6 cells) stained with antibodies according to manufacturer's recommendation (as previously described [40]) in Flow Cytometry Staining buffer (FSB, eBioscience) at room temperature in the dark, then washed twice with FSB. Lymphoid cell infiltration was analyzed with tumor cell suspension assessed in accordance with manufacturer's recommendation (Miltenyi Biotech). Analysis of CD8 + cytotoxic activity was performed using Granzyme labelling of tumor cell suspension plated overnight at 37 °C in 96-well with complete RPMI medium (Dutscher). In the last 4 h, PMA (phorbol 12-myristate 13-acetate; 20 ng/ml; Sigma-Aldrich), ionomycin (1 µg/ml; Sigma-Aldrich), and brefeldin A (2 µl/ml; eBioscience) were added. Assays on lymphoid and myeloid cell infiltration were carried out using Viability Dye eFluor 780 (Thermo Fisher Scientific) to identify cells [40]. Flow cytometry acquisitions were carried out on a Cytoflex 13C cytometer (Beckman Coulter) then the data were analyzed with CytExpert (Beckman Coulter). The identification of lymphoid and

myeloid cells as well as lymphoid cell functionality was performed using gating as previously described [40]. For immunomonitoring results, control animals of RT and PT experiments were pooled together.

RNA extraction, RNA quantification, RNA sequencing and gene set enrichment analysis

Tumor tissues were dissociated using Minilys tissue homogenizer (Bertin, Ozyme) and then total RNA was extracted with Trizol (Invitrogen). Single-end transcriptome reads were pseudo-aligned to the UCSC mm 10 reference genome. The quantification of gene expressions was assessed with the Kallisto algorithm (v 0.44.0) [44] and the program was run with default options.

The analysis of RNA-Seq profiling was achieved with R software (R version 4.2.1). Differential analyses were assessed with the DESeq2 R package (version 1.36.0) [45] using log fold change [46].

Immune cell infiltration in mouse tumor samples was assessed using the *immunedeconv* R package [47]. The mMCPcounter algorithm [48] was applied to TPM-normalized gene expression data to compute immune cell-type-specific scores, representing their abundances in the samples.

Statistical analysis

The results are reported as mean ± SEM (standard error of the mean) for immunomonitoring experiments. Figures were produced using GraphPad Prism software (version 9.2.0; GraphPad Software, USA). Group comparison was assessed using a non-parametric Mann–Whitney test for all immunomonitoring and selected RNA-Seq analyses, while Kaplan Meier curves were analyzed using the Log-rank test. Statistically significance was defined as a p-value < 0.05. For RNA-Seq experiments, gene expression differences were considered significant with an s-value < 0.05 and a log2 fold change ≥ 1 [49]. Gene set enrichment analysis was performed using gprofiler2 (version 0.2.1) [50].

Results

Photon and proton radiation trigger comparable immune response pathways in tumor treatment

RNA-Seq profiling was performed to compare 3 × 8 Gy delivered with photon or proton radiations with non-irradiated CT26 tumors, seven days after the last radiation fraction (Fig. 1A). For each contrast, genes differentially expressed exhibiting a fold change ≥ 2 between the irradiated and non-irradiated conditions were subjected to gprofiler2 to generate a functional enrichment list. Notably, functional enrichments were observed in pathways associated with immune response, as identified in GO, KEGG and REACTOME databases.

RNA-Seq transcriptomic analysis identified 1317 differentially expressed genes between the unirradiated control and 3 × 8 Gy photon-irradiated groups, with a predominant gene overexpression (Fig. 1B). Pathways encompassing the two main types of immune responses were identified, including innate and adaptive immune responses (Fig. 1C). The heatmap derived from the RNA-Seq analysis performed after 3 × 8 Gy proton irradiation represented 1712 differentially expressed genes, with most genes being overexpressed (Fig. 1D). Enrichment analysis of these genes highlighted immune response pathways, mirroring those identified in the RT analysis, comprising adaptive, innate and cytokine immune responses (Fig. 1E). In addition to the primary immune response pathways, transcriptomic analyses identified the activation of pathways associated with cytokine production, T cell receptor signaling, chemokine signaling, and cytokine-cytokine receptor interactions following both photon and proton fractionations (Fig. 1C and E).

Differential regulation of immune signaling genes between PT and RT

Further examination of these genes uncovered the induction of several genes in the interferon type I pathway. Notably, both *cxcl10* and *ifnar* exhibited significant induction after RT and PT (Fig. 1F). Noteworthy is the exclusive induction of trex1 observed specifically after PT treatment (Fig. 1G).

Differences and similarities in tumor infiltration by immune cells after proton or photon irradiation

To characterize immune modifications within the TME following each treatment depicted in Fig. 2A, we employed flow cytometry methodologies using specific lymphoid and myeloid antibody panels.

Tumors treated with either RT or PT displayed a comparable immune response for several parameters, such as a significant influx of CD45 + immune cells within the tumor (Fig. 2B). Among these cells, lymphocytes CD3 + were predominantly represented, exhibiting an increased proportion in the TME following RT (17.6 ± 6.7% of CD3 + /total cells, p = 0.0002) or PT (12.4 ± 9.2% of CD3 + /total cells, p = 0.003) treatment compared to untreated samples (2.9 ± 1.1% of CD3 + /total cells). Notably, the recruitment of CD8 + lymphocytes was heightened after irradiation, with a significantly higher level observed after RT opposed to PT (p = 0.045). Regardless of treatment, a majority of infiltrating CD8 + cells presented an initial level of exhaustion, characterized by PD-1 expression on their surface (CD8 + PD1 +). This level of exhaustion was significantly lower after PT irradiation than RT irradiation with 60.1 ± 25.3% and 83.9 ± 5.0% respectively of

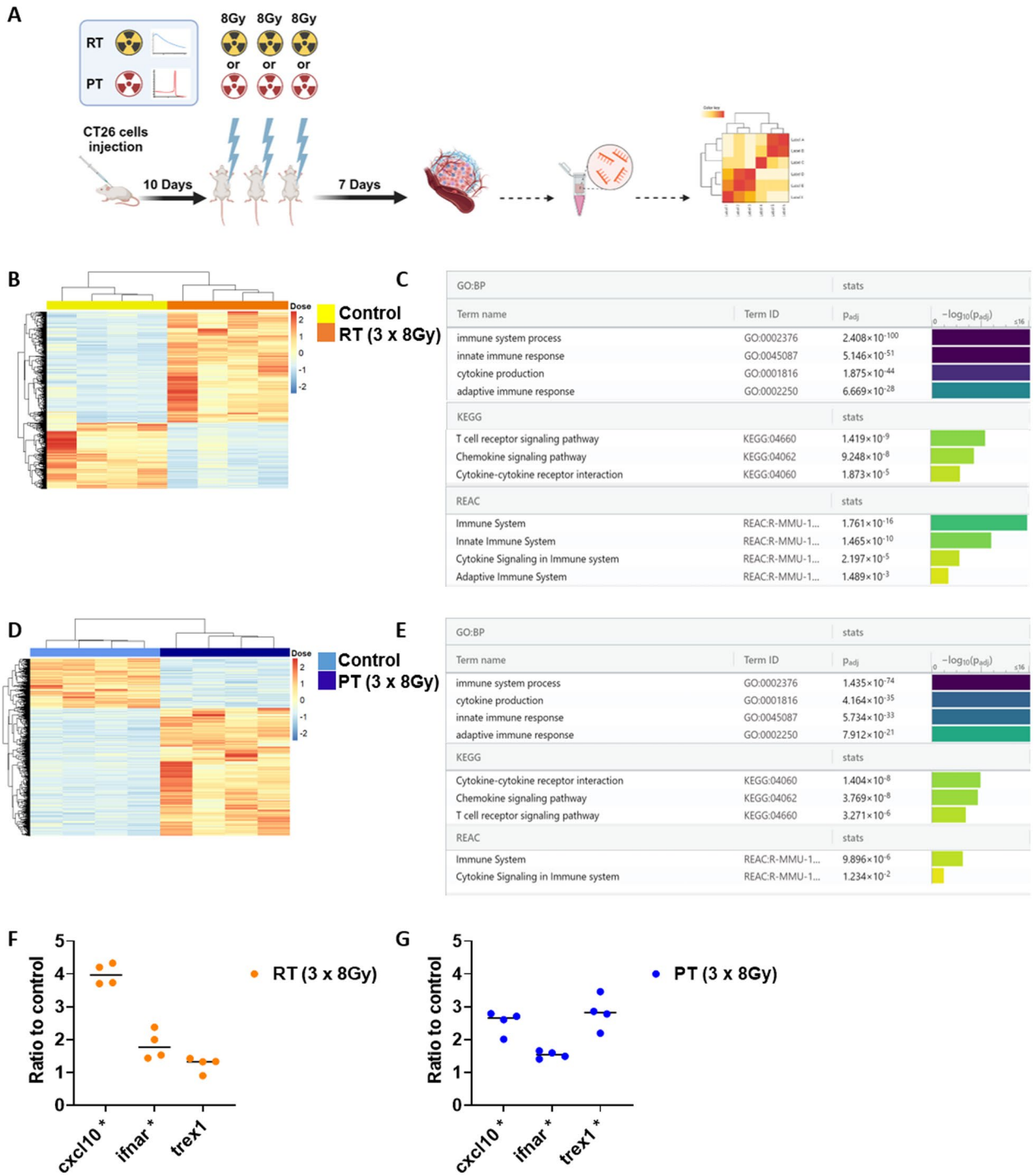

Fig. 1 RNA-Seq profiling analysis was assessed seven days post-irradiation, comparing CT26 tumors treated with 3 × 8 Gy with either RT or PT against non-irradiated controls (Control) (**A**) (Created in BioRender). Heatmaps were constructed to illustrate transcriptomic immune response pathways associated with RT (**B**) or PT (**D**), with statistical significance set a P-value < 0.05 and a fold change ≥ 2 using R software. Each experimental group comprised four mice. Enrichment analysis performed with gProfiler2 yielded lists from the Gene Ontology (GO), Kyoto Encyclopedia of Genes and Genomes (KEGG) and REACTOME databases, associated with immune response pathways subsequent to RT (**C**) or PT (**E**) treatments. Ratio compared to control of the induction of certain interferon pathway genes, including cxcl10, ifnar and trex1 genes was observed following RT (**F**) or PT (**G**) treatments. Statistical analyses were performed using non-parametric Mann–Whitney test. Gene-specific p values are indicated on the graph next to the corresponding gene names. *p < 0.05, n = 4 per group

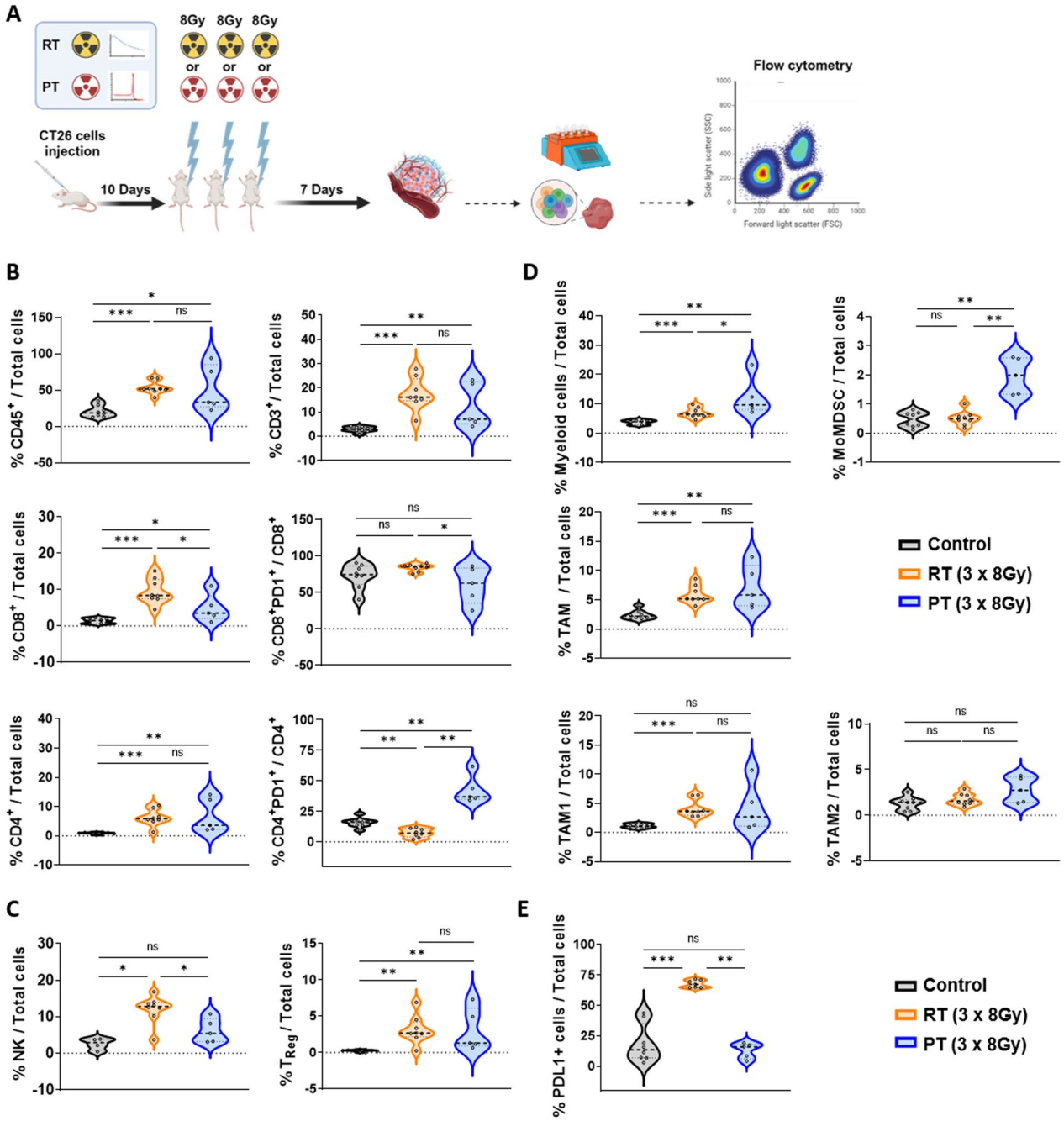

Fig. 2 Tumor microenvironment modifications induced by photon or proton therapy. Comparison of immune cell infiltration in CT26 tumors 7 days after 3×8 Gy with either RT or PT and non-irradiated controls (**A**) (Created in BioRender). The proportion of lymphocyte cells and their exhausted status (**B**) or NK and Treg (**C**), or myeloid cells (**D**) are represented with violin plots. Proportion of all cells expressing PDL1 (**E**). Statistical analyses were performed using non-parametric Mann–Whitney. *p < 0.05, **p < 0.01, ***p < 0.001, n = 5–8 per group

LT CD8 + PD1 + /total LT CD8 + (p = 0.045). Additionally, a significant increase in CD4 + PD1 + T cells was observed in the PT condition. Notably, only RT induced the recruitment of NK cells in the TME (Fig. 2C). Conversely, regardless of the type of irradiation administered, there was a significant increase in the quantity of Treg immunosuppressive cells within the tumor (Fig. 2C). Additionally, a greater proportion of myeloid cells after irradiation, particularly MoMDSC was observed after PT treatment compared to RT

($p = 0.0016$). In a parallel manner between RT and PT, we also observed the induction of TAM infiltration, particularly regarding TAM1 cells after RT (Fig. 2D).

These results are consistent with RNA-Seq data analyses, which revealed a significant increase in lymphocyte infiltration, particularly CD8 + T cells and macrophages, after both PT and RT. In contrast, NK cell infiltration was significantly enhanced only by RT (Figure S1).

Interestingly, only RT treatment induced PD-L1 overexpression (67.7 ± 3.11 vs control 18.5 ± 15.6, $p = 0.0003$) within the TME seven days after radiation, whereas no significant difference in the expression of this protein was observed after PT compared to the control condition (13.0 ± 6.4 and 18.5 ± 15.6 respectively, $p = 0.94$) (Fig. 2E).

Combination of immunotherapy with photons demonstrates enhanced survival compared to its combination with protons

We investigated the efficacy of combining a 3×8 Gy fractionation schedule with concurrent anti-PD-L1 immunotherapy (IT), administered three times per week over three weeks (Fig. 3A). The anti-PD-L1 treatment alone did not induce a significant difference compared to the control (Fig. 3B). Following treatment with photon radiotherapy (RT + IgG), a growth delay was observed, where the tumor volume limit for the entire group was reached between 20–40 days (Fig. 3B). The addition of anti-PD-L1 with RT resulted in a further growth delay, yielding 5 mice in complete response (complete tumor disappearance) out of the 11 animals in the group.

Similar to the analysis conducted with photon, anti-PD-L1 treatment alone did not induce a significant difference compared to the untreated control in the PT experiment (Fig. 3D). Proton therapy treatment (PT + IgG) induced a more pronounced growth delay than RT, with tumors reaching the tumor volume limit between 20–48 days and even 2 mice achieving complete response, consistent with the established effect of PT compared to RT. Combining PT with anti-PD-L1 IT demonstrated an additional enhancement in growth delay, with 4 mice in complete response out of the 10 animals in this group.

Finally, Kaplan Meier analysis with the log-rank test revealed a significant improvement in survival for the combination of RT and anti-PD-L1 IT compared to RT alone ($p = 0.0023$) (Fig. 3C). In contrast, no significant difference in survival was observed with the combination of PT and IT compared to PT alone (Fig. 3E). The lack of a significant survival benefit with the addition of anti-PD-L1 to PT may be attributed to the high antitumor efficacy of PT alone, particularly in comparison to RT, as evidenced by the observation of two complete responses.

Discussion

Photon-based radiotherapy (RT) has been the standard form of radiation therapy for decades. In contrast, proton therapy (PT), first applied clinically in 1954, has faced barriers to widespread adoption due to its high costs and logistical complexities. Nevertheless, increasing demand for precision and safety in cancer treatment has driven a rapid expansion in the use of PT. Concurrently, the integration of RT with immunotherapy (IT) has gained traction as evidenced by over 650 clinical trials currently ongoing or in analysis. Radiation dose, dose rate [51], fractionation schedule [24, 52], ballistic [38] and particle type [34, 40] are key factors influencing immune responses and treatment efficacy. Despite the increasing integration of PT and IT in clinical trials, a systematic evaluation of these parameters and their immunomodulatory effects remains limited. A more detailed mechanistic understanding of radiation-induced immune modulation is essential for optimizing combination strategies. Recently, studies have started to evaluate the combined effectiveness of PT and IT in clinical settings, particularly with anti-PD-1. However, to our knowledge this study is the first to directly compare the intratumoral immune responses elicited by RT and PT, as well as their combined effects with anti-PD-L1 immunotherapy.

Our data indicate that both RT and PT activate immune response pathways. Despite transcriptomic data highlighting the induction of similar molecular pathways, certain differences were observed. Chemokine release after RT and PT attracts immune cells to the treated area, potentially modulating inflammation, influencing the immune responses against tumor cells, and the local vascularization. Both radiation modalities induced a significant upregulation of IFN-inducible chemokines, including *cxcl10*, *cxcl11*, cxcl16, *ccl3*, *ccl4*, *ccl5* and *ccl11*. Additionally, RT induced cxcl9, while PT upregulated *ccl7*, *ccl8*, and *ccl22* (Figure S2). These results align with the findings by Vanpouille-Box et al., who reported an upregulation of IFN-inducible chemokines (*cxcl9*, *cxcl10*, *cxcl11*, *cxcl16 and ccl2* and *ccl5*) after a 3×8 Gy RT treatment on TSA tumors [52], as well as those from other studies [15, 16].

For instance, the expression of *trex1* was analyzed in response to PT and RT. Consistent with prior reports by Vanpouile-Box et al. [52], RT did not significantly modulate *trex1* expression with 8 Gy per fraction, associated with a significant upregulation of type I IFN-related genes such as *cxcl10* and *ifnar* (Fig. 1F) and others (Figure S3A). Interestingly, PT triggered a significant increase in *trex1* expression without inhibition of type I IFN gene expression. Instead, this was accompanied by a concurrent increase in *cxcl10,* albeit to a lesser extent than observed with RT, along with the upregulation of

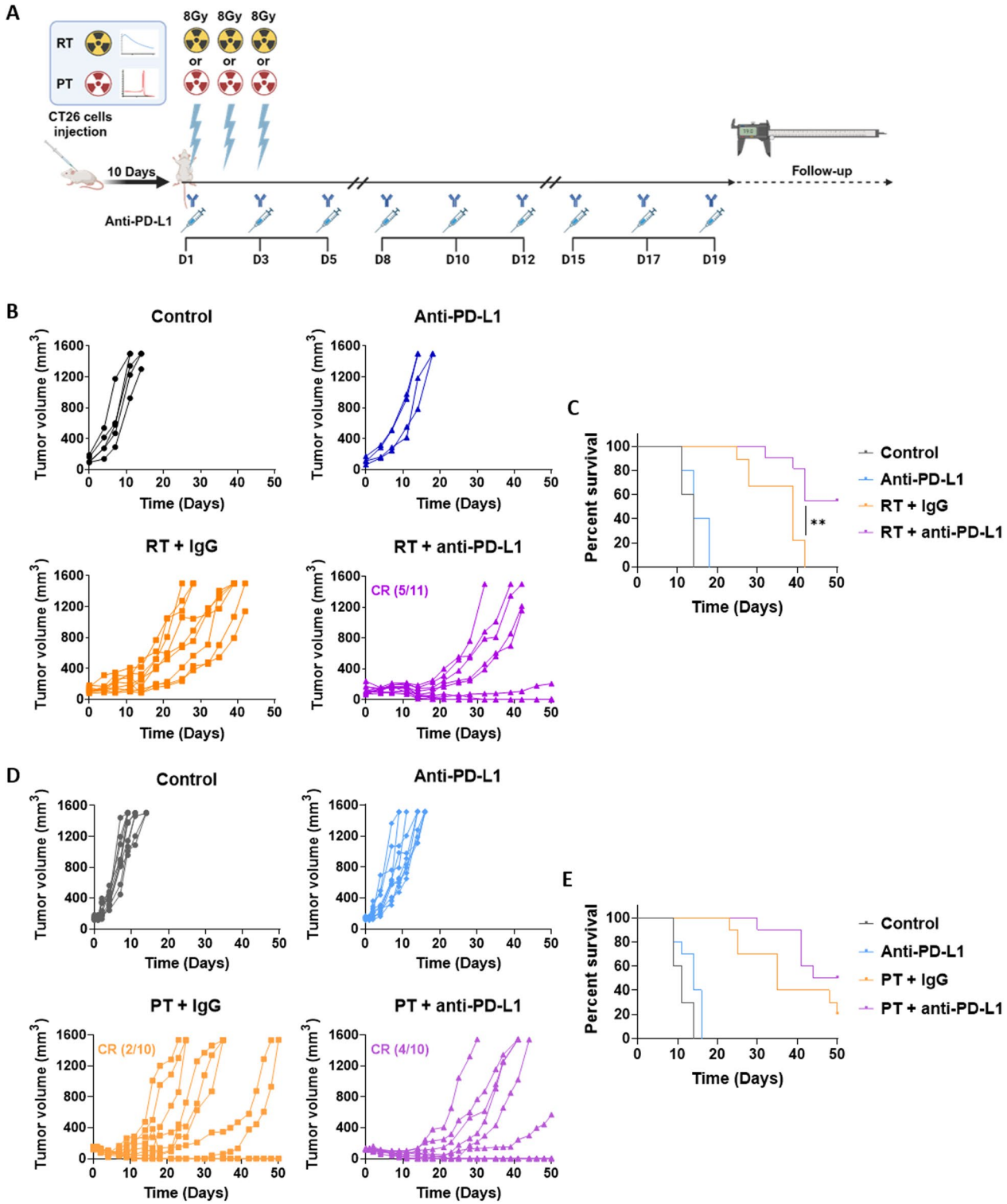

Fig. 3 Efficacy of combination therapy involving anti-PD-L1 treatment with either RT or PT. Tumors were treated with 3 × 8 Gy and anti-PD-L1 (10 mg/kg) 3 times per week over 3 weeks, 3 ten days after the injection of colon CT26 murine cancer cells into Balb/c mice (A) (Created in BioRender). Evaluation of untreated (black) CT26 tumors or those treated with anti-PD-L1 (blue), 3 × 8 Gy delivered with RT or PT irradiation combined with IgG (control) (orange) and RT or PT combined with anti-PD-L1 (purple) on tumor volumes implanted in immunocompetent BALB/c mice (B and D). Kaplan Meier survival curves with log-rank test comparisons, $^{**}p < 0.01$ (C and E). Sample size: n = 5–10 mice per group for RT and n = 10–11 mice per group for PT. CR: complete response

ifnar (Fig. 1G) and other type I IFN-related genes (Figure S3B). TREX1 exonuclease is known to degrade cytosolic DNA fragments, thereby preventing their detection by the cGAS-STING complex and the subsequent activation of the associated pathway leading to the expression of type I IFN genes.

After PT, the increased expression of TREX1 exonuclease could lead to the degradation of cytosolic DNA, thereby reducing cGAS/STING pathway activation and limiting cxcl10 induction. As Cxcl10 recruits T and NK immune cells, its lower expression after PT could explain the more moderate CD8 + T cell infiltration observed compared to RT. This differential Trex1 regulation may result from PT's localized energy deposition within the Bragg peak, leading to highly clustered DNA damage, which has been linked to trex1 upregulation in high-dose irradiation [52, 53]. Additionally, chromatin modification induced by PT, such as changes in DNA methylation and histone pattern could influence trex1 transcription [54]. Given that trex1 negatively regulates the type I IFN response, its upregulation after PT may reduce cxcl10, diminishing immune cell recruitment and explaining the reduced CD8 + T cell infiltration compared to RT.

In addition to RNA-Seq-based analysis of immune cell components, a detailed characterization of the TME was considered essential and was achieved using flow cytometry to precisely identify and quantify individual cell types. Our immunomonitoring investigation presented both similarities and disparities in the immunoactivating and immunosuppressive effects induced by a 3×8 Gy fractionation scheme of RT or PT. Regardless of the particle type used, tumor heating was observed with infiltration of CD45 + immune cells. Among these infiltrating cells, CD8 + lymphocytes, key mediators of the antitumor immune response, were infiltrated consistent with our previous findings reported for the same model using a different fractionation scheme (1×16.4 Gy) [40]. Notably, these CD8 + T cells were less exhausted after PT compared to RT.

Radiation-induced antitumor responses have been widely shown to depend primarily on CD8 + T lymphocytes [15]. Moreover, the extent of CD8 + T cell infiltration in tumors has been linked to treatment efficacy and patient survival outcomes [55]. Therefore, evaluating CD8 + T cell infiltration after RT, in conjunction with the induction of cxcl10 expression may serve as a potential biomarker for predicting response to RT, particularly when combined with IT.

Interestingly, we observed a significant infiltration of NK cells only after RT irradiation. This infiltration could be linked to a significant increase in *cxcl9* gene expression detected after RT but not after PT. This lack of induction of *cxcl9* expression after PT could be also related to less CD8 + T cell infiltration after PT since this chemokine is involved in the attraction of both cell types [56]. Concerning the immunosuppressive response activation, we observed an increase in the infiltration of Treg cells after both RT and PT. Those results are consistent with those previously reported by our team [24] using the same RT scheme and cancer model. Hu et al. also reported the infiltration of both CD8 + T cells and Tregs after PT [57]. We also observed an increase in the infiltration of myeloid distinct-derived suppressor cells (MDSCs) only after PT. This observation was similarly documented by Chen et al. following a single dose of 12 Gy PT [58]. MDSCs possess a number of immunosuppressive properties, acting on various tumor response players such as inhibition of recruitment, activation and functionality of antitumor T cells. By secreting IL-10 and TGF-beta, MDSCs also limit NK and macrophage function [59]. Recently, we demonstrated that this immunosuppressive response can be effectively inhibited by combining treatment with low-dose 5-fluorouracil, which induces MDSC death without direct cytotoxic effects on tumor cells [60]. This strategy highlights the potential of such chemotherapy combination with 3×8 Gy PT to limit the immunosuppressive response and improve effectiveness of the treatment.

Our immunomonitoring study suggested a potential advantage of immunoactivation through RT over PT in modulating the TME, with increased CD8 + T cell infiltration observed after RT and enhanced MDSCs infiltration after PT. The 3×8 Gy fractionation regimen in PT demonstrates greater efficacy compared to RT alone. This disparity may be explained by differences in the relative biological effectiveness (RBE) between PT and RT. In our study, the ballistic advantage of PT is not evident, as the RT approach employed ensures precise tumor targeting while entirely sparing the OAR and the rest of the mouse's body. This level of precision is not typically achievable in clinical RT practice, introducing a potential bias in our RT model when compared to clinical applications. Specifically, our RT treatment plan accounts for ballistic effects by exclusively sparing the mouse and directing radiation solely towards the tumor. Recent findings by Tadepalli et al. have demonstrated the importance of ballistic considerations in a comparative analysis in a conformal radiation therapy (CRT) plan, similar to our ballistic, and a stereotactic radiation therapy (SRT) plan, which irradiates a portion of the mouse's healthy organs in a manner more representative of clinical conditions [38]. This disparity resulted in a more pronounced immunosuppressive response and monocytes infiltration in the irradiated OAR. In contrast, the ballistic characteristics of PT are more aligned with clinical conditions, particularly with the absence of dose deposition behind the tumor, attributable to the Bragg peak [61]. In the

clinical setting, the advantage of PT in sparing OAR, which correlates with lymphocyte infiltration, appears to be linked to immune efficacy on lymphopenia compared to RT [39]. Thus, there is certainly an interest in combining PT with IT, with careful adaptation of optimal IT targets, adjusted radiation fractionations, and tailored IT and PT sequences.

Previously we have demonstrated, using the same tumor model that the induction of target expression (PD-L1 or TIGIT) by RT correlated with the efficacy of combination immunotherapy [24]. While an induction of PD-L1 was evidenced seven days following RT, such induction was not observed after PT. Regarding the lack of enhanced PD-L1 expression following PT, Chen et al. observed an induction/upregulation of this expression in a hepatocellular carcinoma model irradiated at a single dose of 12 Gy, specifically during the early post-PT phase at day 3, but no longer observed at day 12 [58]. In relation to the lack of benefit observed with anti-PD-L1 in combination with PT, in a subcutaneous model of hepatocellular carcinoma, Chen et al. observed a gain at day 12 but did not extend the efficacy study beyond this time point [58]. However, in an orthotopic model, IT did not provide additional efficacy compared to PT alone (12 Gy), also assessed at day 12. This underscores the importance of conducting a more prolonged follow-up to thoroughly evaluate long-term outcomes. In our present study, the combination of RT and IT demonstrated a significant improvement compared to RT alone, while PT and IT were not significantly different from PT alone. The lack of a significant survival difference between PT alone versus PT combined with anti-PDL1 may be also due to the high antitumor efficacy of PT alone, which potentially limits an additional benefit of the PT and IT combination, particularly in contrast to RT.

Few clinical trials are terminated or currently underway combining PT with IT and these combinations are often limited to traditional or historical IT such as anti-PD1 (NCT03764787, NCT03539198 and NCT03765190), anti-PD-L1 (NCT032677836, NCT03450967) and anti-CTLA4 (NCT03450967). Given the radio-induced immune response associated with PT in our model, there is potential interest in co-administering PT with an inhibitor of MDSC, like 5-fluorouracil and/or an inhibitor of Treg, such as CTLA-4 or cyclophosphamide. Additionally, our RNA-Seq analysis revealed a substantial upregulation of targets such as *tigit, lag-3, havcr2* and *cd40* after PT (Figure S4) suggesting the potential for evaluating the efficacy of PT in combination with IT targeting these proteins.

In conclusion, we have provided in our original study the impact of PT versus RT on the intratumoral immune response. While both modalities elicit similar radiation-induced immune effects, notable differences were observed, particularly in the immunosuppressive response. These findings highlight the need to optimize the selection of immunotherapies combined with PT to achieve an optimal therapeutic outcome. Our results indicate promising immunotherapy strategies. It would be beneficial to explore more recent immunotherapies or those currently in development, to select therapies based on the induction of target expression. Like in the combination of IT with RT, optimizing the PT dose, fractionation and combination sequences is also crucial for maximizing treatment efficacy of PT and IT.

Abbreviations

CRT	Conformal radiation therapy
DAMPs	Danger-associated molecular patterns
GO	Gene ontology
IFN-γ	Interferon gamma
IgG	Immunoglobulin G
IT	Immunotherapy
KEGG	Kyoto encyclopedia of genes and genomes
LET	Linear energy transfer
MDSCs	Myeloid-derived suppressive cells
NK	Natural killer
OAR	Organs at risk
PD-1	Programmed cell death protein 1
PD-L1	Programmed death-ligand 1
PT	Proton therapy
ROS	Reactive oxygen species
RT	Radiotherapy
SRT	Stereotactic radiation therapy
TAM-2	Tumor-associated macrophages 2
TME	Tumor microenvironment
Treg	Regulatory T cells
TV	Tumor volume

Supplementary Information

The online version contains supplementary material available at https://doi.org/10.1186/s12967-025-06377-7.

Suppementary Material 1: Fig. 1 Deconvolution of RNA-Seq data to estimate the relative abundance of T cells, CD8+ T cells, NK cells, and macrophage/monocyte populations. Statistical analyses were performed using non-parametric Mann-Whitney test. n = 4 per group. Fig. 2 Heatmaps illustrating the ccl and cxcl chemokines and cytokines associated with RT or PT. Statistical significance was determined with a P-value < 0.05 and a fold change ≥ 2, analyzed using R software. n = 4 per group. Fig. 3 Expression of some type-I interferon genes after RT and PT compared to their respective non-irradiated controls. Statistical analyses were performed using non-parametric Mann-Whitney test. Gene-specific p values are indicated on the graph next to the corresponding gene names. *p<0.05, n = 4 per group. Fig. 4 Expression of Tigit, Lag3, Havcr2, cd40, and Pdcd1following RT and PT compared to their respective non-irradiated controls. Statistical analyses were performed using non-parametric Mann-Whitney test. Gene-specific p values are indicated on the graph next to the corresponding gene names. *p<0.05, n = 4 per group

Acknowledgements

We acknowledge M. Pellicoli and J. Schuler (IPHC, UMR7178) for their technical support with the cyclotron CYRCé and L. Thomas and B. Jessel for their technical support in the animal care facility (IPHC, UMR7178).

Author contributions

H.B. and C.Mi wrote and edited this manuscript. H.B., C.Mi. and G.N. were involved in the conceptualization and the methodology design of the study.

H.B., V.M., L.F., C.Mu. and C.Mi. performed the tumor-grafts, evaluated the tumor volume and organized the animal care procedures. C.Mu., H.B. and M.R. prepared for the proton therapy sessions and implementation. E.L., V.M., F.F., P.A.L., F.G. and C.Mi. performed the immuno-monitoring analysis by flow cytometry. R.B. performed the RNA sequencing and A.N. and C.R. analyzed all RNA sequencing data. H.B. and C.Mi. supervised the project. H.B., C.Mi. and A.N performed the statistical analysis of the study. H.B., C.Mi., A.N., J.B-G., C.R. and E.L. had access to the raw data, analyzed and interpreted the data. H.B., C.Mi., A.N. and E.L. participated in writing the manuscript. J.B-G. and G.N. were involved in the proofreading and revision of the manuscript. All authors have read, corrected and agreed to the published version of the manuscript.

Funding
This study was supported by Ligue Régionale contre le Cancer, CCIRGE, Centre Georges-François Leclerc, Centre Paul Strauss and Conseil Régional Bourgogne Franche-Comté.

Availability of data and materials
The datasets used and/or analyzed during the current study are available from the corresponding author on reasonable request.

Declarations

Ethics approval and consent to participate
The animal experiments were carried out according to established protocols approved under French legislation governing the utilization of laboratory animals (EU Directive 2010/63/EU for animal experiments), and adhered to ethical rules for the care and use of animals for research from the small animal ethics committee (C2ea Grand Campus n°105 and C2ea Cremeas n°35, C2ea Icomech n°38) and the French Ministries of Research and Agriculture (APAFIS#13961-2018022215413276 v2, APAFIS#22350-201910091738155 v2 and APAFIS#8235-201612161350414_v1).

Consent for publication
Not applicable.

Competing interests
The authors declare no conflict of interest.

Author details
[1]Radiobiology Laboratory, Paul Strauss Comprehensive, Cancer Center, Institut de Cancérologie Strasbourg Europe (ICANS), UNICANCER, 67000 Strasbourg, France. [2]Equipe Imagerie Multimodale Intégrative en Santé, ICube, UMR7357, Université de Strasbourg, Strasbourg, France. [3]Institut Pluridisciplinaire Hubert Curien, Université de Strasbourg, CNRS, UMR 7178, 67200 Strasbourg, France. [4]X-Rain: Research Unit in Radiotherapy Combined with Immunotherapies and Nanoparticles, IMATHERA, Department of Radiation Oncology, Unicancer-Georges-Francois Leclerc Cancer Center, 21000 Dijon, France. [5]Molecular Biology Clinical Research, Unicancer–Center Georges-Francois Leclerc, 21000 Dijon, France. [6]CTM, INSERM, UMR 1231, Trecs Team, CTM, 21000 Dijon, France. [7]PTBC, CGFL, Dijon, France. [8]Institut de Cancérologie Strasbourg Europe (ICANS), Paul Strauss Comprehensive Cancer Center, Department of Radiation Oncology, UNICANCER, 17 Rue Albert Calmette, 67200 Strasbourg, France.

Received: 31 December 2024 Accepted: 12 March 2025
Published online: 23 March 2025

References

1. Berger T, Noble DJ, Shelley LEA, Hopkins KI, McLaren DB, Burnet NG, et al. 50 years of radiotherapy research: evolution, trends and lessons for the future. Radiother Oncol. 2021;165:75–86.
2. Mercadante S. Breakthrough cancer pain in the radiotherapy setting: a systematic and critical review. Exp Rev Anticancer Ther. 2023;23(3):229–34.
3. Bernier J, Hall EJ, Giaccia A. Radiation oncology: a century of achievements. Nat Rev Cancer. 2004;4(9):737–47.
4. Galluzzi L, Yamazaki T, Kroemer G. Linking cellular stress responses to systemic homeostasis. Nat Rev Mol Cell Biol. 2018;19(11):731–45.
5. Rodriguez-Ruiz ME, Vitale I, Harrington KJ, Melero I, Galluzzi L. Immunological impact of cell death signaling driven by radiation on the tumor microenvironment. Nat Immunol. 2020;21(2):120–34.
6. Cho H, Kim JE, Hong YS, Kim SY, Kim J, Ryu YM, et al. Comprehensive evaluation of the tumor immune microenvironment and its dynamic changes in patients with locally advanced rectal cancer treated with preoperative chemoradiotherapy: from the phase II ADORE study. Oncoimmunology. 2022;11(1):2148374.
7. Lhuillier C, Rudqvist NP, Elemento O, Formenti SC, Demaria S. Radiation therapy and anti-tumor immunity: exposing immunogenic mutations to the immune system. Genom Med. 2019;11(1):40.
8. Boustani J, Grapin M, Laurent PA, Apetoh L, Mirjolet C. The 6th R of radiobiology: reactivation of anti-tumor immune response. Cancers (Basel). 2019. https://doi.org/10.3390/cancers11060860.
9. Dewan MZ, Galloway AE, Kawashima N, Dewyngaert JK, Babb JS, Formenti SC, et al. Fractionated but not single-dose radiotherapy induces an immune-mediated abscopal effect when combined with anti-CTLA-4 antibody. Clin Cancer Res. 2009;15(17):5379–88.
10. McLaughlin M, Patin EC, Pedersen M, Wilkins A, Dillon MT, Melcher AA, et al. Inflammatory microenvironment remodelling by tumour cells after radiotherapy. Nat Rev Cancer. 2020;20(4):203–17.
11. Vanpouille-Box C, Formenti SC, Demaria S. Toward precision radiotherapy for use with immune checkpoint blockers. Clin Cancer Res. 2018;24(2):259–65.
12. Lopez-Pelaez M, Young L, Vazquez-Chantada M, Nelson N, Durant S, Wilkinson RW, et al. Targeting DNA damage response components induces enhanced STING-dependent type-I IFN response in ATM deficient cancer cells and drives dendritic cell activation. Oncoimmunology. 2022;11(1):2117321.
13. Tubin S, Yan W, Mourad WF, Fossati P, Khan MK. The future of radiation-induced abscopal response: beyond conventional radiotherapy approaches. Fut Oncol. 2020;16(16):1137–51.
14. Demaria S, Formenti SC. The abscopal effect 67 years later: from a side story to center stage. Br J Radiol. 2020;93(1109):20200042.
15. Dovedi SJ, Adlard AL, Lipowska-Bhalla G, McKenna C, Jones S, Cheadle EJ, et al. Acquired resistance to fractionated radiotherapy can be overcome by concurrent PD-L1 blockade. Cancer Res. 2014;74(19):5458–68.
16. Laurent PA, Morel D, Meziani L, Depil S, Deutsch E. Radiotherapy as a means to increase the efficacy of T-cell therapy in solid tumors. Oncoimmunology. 2023;12(1):2158013.
17. Wennerberg E, Galluzzi L. Born to kill: NK cells go to war against cancer. Trends Cancer. 2019;5(3):143–5.
18. Mirjolet C, Baude J, Galluzzi L. Dual impact of radiation therapy on tumor-targeting immune responses. Int Rev Cell Mol Biol. 2023. https://doi.org/10.1016/S1937-6448(23)00114-4.
19. Jimenez-Cortegana C, Galassi C, Klapp V, Gabrilovich DI, Galluzzi L. Myeloid-derived suppressor cells and radiotherapy. Cancer Immunol Res. 2022;10(5):545–57.
20. Charpentier M, Spada S, Van Nest SJ, Demaria S. Radiation therapy-induced remodeling of the tumor immune microenvironment. Semin Cancer Biol. 2022;86(Pt 2):737–47.
21. Cytlak UM, Dyer DP, Honeychurch J, Williams KJ, Travis MA, Illidge TM. Immunomodulation by radiotherapy in tumour control and normal tissue toxicity. Nat Rev Immunol. 2022;22(2):124–38.
22. De Martino M, Daviaud C, Diamond JM, Kraynak J, Alard A, Formenti SC, et al. Activin a promotes regulatory T-cell-mediated immunosuppression in irradiated breast cancer. Cancer Immunol Res. 2021;9(1):89–102.
23. Ruckert M, Flohr AS, Hecht M, Gaipl US. Radiotherapy and the immune system: more than just immune suppression. Stem Cell. 2021;39(9):1155–65.
24. Grapin M, Richard C, Limagne E, Boidot R, Morgand V, Bertaut A, et al. Optimized fractionated radiotherapy with anti-PD-L1 and anti-TIGIT: a promising new combination. J Immunother Cancer. 2019;7(1):160.
25. Dovedi SJ, Illidge TM. The antitumor immune response generated by fractionated radiation therapy may be limited by tumor cell adaptive resistance and can be circumvented by PD-L1 blockade. Oncoimmunology. 2015;4(7): e1016709.
26. Chi A, Nguyen NP. Mechanistic rationales for combining immunotherapy with radiotherapy. Front Immunol. 2023;14:1125905.

27. Zhang Z, Liu X, Chen D, Yu J. Radiotherapy combined with immunotherapy: the dawn of cancer treatment. Signal Transduct Target Ther. 2022;7(1):258.
28. Chargari C, Levy A, Paoletti X, Soria JC, Massard C, Weichselbaum RR, et al. Methodological development of combination drug and radiotherapy in basic and clinical research. Clin Cancer Res. 2020;26(18):4723–36.
29. Boustani J, Lecoester B, Baude J, Latour C, Adotevi O, Mirjolet C, et al. Anti-PD-1/Anti-PD-L1 drugs and radiation therapy: combinations and optimization strategies. Cancers (Basel). 2021. https://doi.org/10.3390/cancers13194893.
30. Roussot N, Fumet JD, Limagne E, Thibaudin M, Hervieu A, Hennequin A, et al. A phase I study of the combination of atezolizumab, tiragolumab, and stereotactic body radiation therapy in patients with metastatic multiorgan cancer. BMC Cancer. 2023;23(1):1080.
31. Demaria S, Guha C, Schoenfeld J, Morris Z, Monjazeb A, Sikora A, et al. Radiation dose and fraction in immunotherapy: one-size regimen does not fit all settings, so how does one choose? J Immunother Cancer. 2021. https://doi.org/10.1136/jitc-2020-002038.
32. Deutsch E, Chargari C, Galluzzi L, Kroemer G. Optimising efficacy and reducing toxicity of anticancer radioimmunotherapy. Lancet Oncol. 2019;20(8):e452–63.
33. Palermo B, Bottero M, Panetta M, Faiella A, Sperduti I, Masi S, et al. Stereotactic ablative radiation therapy in 3 fractions induces a favorable systemic immune cell profiling in prostate cancer patients. Oncoimmunology. 2023;12(1):2174721.
34. Helm A, Totis C, Durante M, Fournier C. Are charged particles a good match for combination with immunotherapy? Current knowledge and perspectives. Int Rev Cell Mol Biol. 2023;376:1–36.
35. Zhou H, Tu C, Yang P, Li J, Kepp O, Li H, et al. Carbon ion radiotherapy triggers immunogenic cell death and sensitizes melanoma to anti-PD-1 therapy in mice. Oncoimmunology. 2022;11(1):2057892.
36. Mohan R, Grosshans D. Proton therapy—present and future. Adv Drug Deliv Rev. 2017;109:26–44.
37. Yuan TZ, Zhan ZJ, Qian CN. New frontiers in proton therapy: applications in cancers. Cancer Commun (Lond). 2019;39(1):61.
38. Tadepalli S, Clements DR, Saravanan S, Arroyo Hornero R, Ludtke A, Blackmore B, et al. Rapid recruitment and IFN-I-mediated activation of monocytes dictate focal radiotherapy efficacy. Sci Immunol. 2023;8(84):eadd7446.
39. Wang X, Hobbs B, Gandhi SJ, Muijs CT, Langendijk JA, Lin SH. Current status and application of proton therapy for esophageal cancer. Radiother Oncol. 2021;164:27–36.
40. Mirjolet C, Nicol A, Limagne E, Mura C, Richard C, Morgand V, et al. Impact of proton therapy on antitumor immune response. Sci Rep. 2021;11(1):13444.
41. Mirjolet C, Ladjohounlou R, Baude J, Bessieres I. Novel platform for subcutaneous tumor irradiation in mice. Method Cell Biol. 2023;180:69–80.
42. Constanzo J, Vanstalle M, Finck C, Brasse D, Rousseau M. Dosimetry and characterization of a 25-MeV proton beam line for preclinical radiobiology research. Med Phys. 2019;46(5):2356–62.
43. Vanstalle M, Constanzo J, Karakaya Y, Finck C, Rousseau M, Brasse D. Analytical dose modeling for preclinical proton irradiation of millimetric targets. Med Phys. 2018;45(1):470–8.
44. Bray NL, Pimentel H, Melsted P, Pachter L. Near-optimal probabilistic RNA-seq quantification. Nat Biotechnol. 2016;34(5):525–7.
45. Love MI, Huber W, Anders S. Moderated estimation of fold change and dispersion for RNA-seq data with DESeq2. Genome Biol. 2014;15(12):550.
46. Zhu A, Ibrahim JG, Love MI. Heavy-tailed prior distributions for sequence count data: removing the noise and preserving large differences. Bioinformatics. 2019;35(12):2084–92.
47. Merotto L, Sturm G, Dietrich A, List M, Finotello F. Making mouse transcriptomics deconvolution accessible with immunedeconv. Bioinform Adv. 2024. https://doi.org/10.1093/bioadv/vbae032.
48. Petitprez F, Levy S, Sun CM, Meylan M, Linhard C, Becht E, et al. The murine microenvironment cell population counter method to estimate abundance of tissue-infiltrating immune and stromal cell populations in murine samples using gene expression. Genome Med. 2020;12(1):86.
49. Stephens M. False discovery rates: a new deal. Biostatistics. 2017;18(2):275–94.
50. Raudvere U, Kolberg L, Kuzmin I, Arak T, Adler P, Peterson H, et al. g:Profiler: a web server for functional enrichment analysis and conversions of gene lists (2019 update). Nucl Acid Res. 2019;47(W1):W191–8.
51. Laurent PA, Kownacka A, Boidot R, Richard C, Limagne E, Morgand V, et al. In-vivo and in-vitro impact of high-dose rate radiotherapy using flattening-filter-free beams on the anti-tumor immune response. Clin Transl Radiat Oncol. 2020;24:116–22.
52. Vanpouille-Box C, Alard A, Aryankalayil MJ, Sarfraz Y, Diamond JM, Schneider RJ, et al. DNA exonuclease Trex1 regulates radiotherapy-induced tumour immunogenicity. Nat Commun. 2017;8:15618.
53. Radstake WE, Parisi A, Miranda S, Gautam K, Vermeesen R, Rehnberg E, et al. Radiation-induced DNA double-strand breaks in cortisol exposed fibroblasts as quantified with the novel foci-integrated damage complexity score (FIDCS). Sci Rep. 2024;14(1):10400.
54. Fang L, Ying S, Xu X, Wu D. TREX1 cytosolic DNA degradation correlates with autoimmune disease and cancer immunity. Clin Exp Immunol. 2023;211(3):193–207.
55. Pages F, Mlecnik B, Marliot F, Bindea G, Ou FS, Bifulco C, et al. International validation of the consensus Immunoscore for the classification of colon cancer: a prognostic and accuracy study. Lancet. 2018;391(10135):2128–39.
56. Ozga AJ, Chow MT, Luster AD. Chemokines and the immune response to cancer. Immunity. 2021;54(5):859–74.
57. Hu Y, Paris S, Sahoo N, Bertolet G, Wang Q, Wang Q, et al. Nanoparticle-enhanced proton beam immunoradiotherapy drives immune activation and durable tumor rejection. JCI Insight. 2023. https://doi.org/10.1172/jci.insight.167749.
58. Chen MF, Chen PT, Hsieh CC, Wang CC. Effect of proton therapy on tumor cell killing and immune microenvironment for hepatocellular carcinoma. Cells. 2023. https://doi.org/10.3390/cells12020332.
59. Wang S, Zhao X, Wu S, Cui D, Xu Z. Myeloid-derived suppressor cells: key immunosuppressive regulators and therapeutic targets in hematological malignancies. Biomark Res. 2023;11(1):34.
60. Boustani J, Lecoester B, Baude J, Latour C, Limagne E, Ladjohoulou R, et al. Targeting two radiation-induced immunosuppressive pathways to improve the efficacy of normofractionated radiation therapy in a preclinical colorectal cancer model. Int J Radiat Biol. 2024;100(6):912–21.
61. Baude J, Limagne E, Ladjohounlou R, Mirjolet C. Combining radiotherapy and NK cell-based therapies: the time has come. Int Rev Cell Mol Biol. 2023;378:31–60.

Publisher's Note